

CMIP6 skill at predicting interannual to multi-decadal summer monsoon precipitation variability

Article

Accepted Version

Creative Commons: Attribution 4.0 (CC-BY)

Open Access

Monerie, P.-A. ORCID: <https://orcid.org/0000-0002-5304-9559>,
Robson, J. I. ORCID: <https://orcid.org/0000-0002-3467-018X>,
Ndiaye, C. D., Song, C. and Turner, A. G. ORCID:
<https://orcid.org/0000-0002-0642-6876> (2023) CMIP6 skill at
predicting interannual to multi-decadal summer monsoon
precipitation variability. *Environmental Research Letters*, 18
(9). 094002. ISSN 1748-9326 doi:
<https://doi.org/10.1088/1748-9326/acea96> Available at
<https://centaur.reading.ac.uk/112717/>

It is advisable to refer to the publisher's version if you intend to cite from the work. See [Guidance on citing](#).

To link to this article DOI: <http://dx.doi.org/10.1088/1748-9326/acea96>

Publisher: Institute of Physics

All outputs in CentAUR are protected by Intellectual Property Rights law, including copyright law. Copyright and IPR is retained by the creators or other copyright holders. Terms and conditions for use of this material are defined in the [End User Agreement](#).

www.reading.ac.uk/centaur

CentAUR

Central Archive at the University of Reading

Reading's research outputs online

ACCEPTED MANUSCRIPT • OPEN ACCESS

CMIP6 skill at predicting interannual to multi-decadal summer monsoon precipitation variability

To cite this article before publication: Paul-Arthur Monerie *et al* 2023 *Environ. Res. Lett.* in press <https://doi.org/10.1088/1748-9326/acea96>

Manuscript version: Accepted Manuscript

Accepted Manuscript is “the version of the article accepted for publication including all changes made as a result of the peer review process, and which may also include the addition to the article by IOP Publishing of a header, an article ID, a cover sheet and/or an ‘Accepted Manuscript’ watermark, but excluding any other editing, typesetting or other changes made by IOP Publishing and/or its licensors”

This Accepted Manuscript is © 2023 The Author(s). Published by IOP Publishing Ltd.



As the Version of Record of this article is going to be / has been published on a gold open access basis under a CC BY 4.0 licence, this Accepted Manuscript is available for reuse under a CC BY 4.0 licence immediately.

Everyone is permitted to use all or part of the original content in this article, provided that they adhere to all the terms of the licence <https://creativecommons.org/licenses/by/4.0>

Although reasonable endeavours have been taken to obtain all necessary permissions from third parties to include their copyrighted content within this article, their full citation and copyright line may not be present in this Accepted Manuscript version. Before using any content from this article, please refer to the Version of Record on IOPscience once published for full citation and copyright details, as permissions may be required. All third party content is fully copyright protected and is not published on a gold open access basis under a CC BY licence, unless that is specifically stated in the figure caption in the Version of Record.

View the [article online](#) for updates and enhancements.

CMIP6 skill at predicting interannual to multi-decadal summer monsoon precipitation variability

Paul-Arthur Monerie^{1*}, Jon I Robson¹, Cassien D Ndiaye^{2,3}, Cenyao Song⁴, Andrew G Turner^{1,5}.

¹ National Centre for Atmospheric Science, Reading, United Kingdom

² LPAO-SF/Cheikh Anta Diop University, Dakar, Senegal

³ LOCEAN/IPSL/Sorbonne University, Paris, France

⁴ Previously at Department of Meteorology, University of Reading, Reading, United Kingdom

⁵ Department of Meteorology, University of Reading, Reading, United Kingdom

*Author to whom any correspondence should be addressed.

Paul-Arthur Monerie; <https://orcid.org/0000-0002-5304-9559>. p.monerie@reading.ac.uk

Jon I Robson; <https://orcid.org/0000-0002-3467-018X>

Cassien D. Ndiaye; <https://orcid.org/0000-0002-7091-1438>

Cenyao Song

Andrew G Turner; <https://orcid.org/0000-0002-0642-6876>

Keywords: summer monsoon precipitation; prediction systems; skill; interannual variability; multi-decadal variability

Abstract

Monsoons affect the economy, agriculture, and human health of two thirds of the world's population. Therefore, predicting variations in monsoon precipitation is societally important. We explore the ability of climate models from the 6th phase of the Climate Model Intercomparison Project (CMIP6) to predict summer monsoon precipitation variability by using hindcasts from the Decadal Climate Prediction Project (Component A). The multi-model ensemble-mean shows significant skill at predicting summer monsoon precipitation from one year to 6-9 years ahead. However, this skill is dependent on the model, monsoon domain, and lead-time. In general, the skill of the multi-model ensemble-mean prediction is low in year 1 but increases for longer-lead times and is largely consistent with externally forced changes. The best captured region is northern Africa for the 2-5- and 6-9-year forecast lead times. In contrast, there is no significant skill using the ensemble-mean over East and South Asia and, furthermore, there is significant spread in skill among models for these domains. By sub-sampling the ensemble we show that the difference in skill between models is tied to the simulation of the externally forced response over East and South Asia, with models with a more skilful forced response capable of better predictions. A further contribution is from skilful prediction of Pacific Ocean temperatures for the South Asian summer monsoon at longer lead-times. Therefore, these results indicate that predictions of the East and South Asian monsoons could be significantly improved.

1. Introduction

Two thirds of the world's population lives in areas where there is a monsoon in summer (Wang & Ding, 2006). Monsoon precipitation variability has effects on economies, agriculture, and human health, among other sectors. Therefore, predicting the future evolution of monsoon precipitation is important, for adaptation strategies (*e.g.*, infrastructure planning).

Individual predictions systems have shown skill at predicting monsoon precipitation on a large range of time scales (Dunstone et al. 2020; Monerie et al. 2021). Regionally, some skill has been found over East and southern Africa (Beraki et al., 2013; Monerie et al., 2018; Walker et al., 2019), South America (Jones et al., 2012), Australia (King et al., 2020), India (Chevuturi et al., 2021; Johnson et al., 2017) and southern China (Lu et al., 2017) at a seasonal time scale. On longer time scales, prediction systems have exhibited substantial skill at predicting decadal variations in Sahel precipitation (Gaetani & Mohino, 2013; Martin & Thorncroft, 2014; Mohino et al., 2016; Ndiaye et al., 2022; Otero et al., 2016; Sheen et al., 2017).

There are multiple sources of skill for predicting summer monsoon precipitation. The role of sea surface temperatures (SSTs), among other slowly varying lower boundary conditions, in predicting monsoon precipitation variations, was theorised by Charney and Shukla (1981). On seasonal time scales, it was shown that the El Niño Southern Oscillation (ENSO) is key for providing skill at predicting precipitation over the tropics (Dunstone et al., 2020; Shukla & Paolino, 1983; Sohn et al., 2019; Wang et al., 2018). On decadal time scales, the North Atlantic and Indian Ocean SSTs also yield a certain amount of predictability for monsoon precipitation (Mohino et al., 2016; Wang et al., 2018), due to the high prediction skill of prediction systems for Atlantic and Indian Ocean sea surface temperature (García-Serrano et al., 2015; Guemas et al., 2013) and to the effects of these oceanic basins on monsoon precipitation.

Anthropogenic forcing is a source of prediction skill for global mean surface air temperature (Boer et al., 2016) and SST (*e.g.*, Guemas et al. 2013) and has known effects on summer monsoon precipitation worldwide (Marvel et al. 2020; Monerie et al. 2022).

Previous studies have quantified skill at predicting monsoon precipitation on multi-year time scales with a small number of climate models and ensemble members (*e.g.*, Bellucci et al. 2015). However, prediction skill values increases with ensemble size (Smith et al., 2019) and we therefore use the large ensemble of the Decadal Climate Prediction Project (DCPP; Boer et al. 2016), reducing unpredictable noise, and providing a better estimate of prediction skill. The large ensemble facilitates understanding of the causes of differences between prediction systems at predicting monsoon precipitation, including structural differences between prediction systems. No robust evaluation across a range of models, monsoon domains and timescales has been provided so far. We thus provide, for the first time, a quantification of the ability of CMIP6 prediction systems at predicting interannual to decadal summer monsoon precipitation variability in a global monsoon framework. We expect skill at predicting summer monsoon precipitation to be model dependent (as shown

1
2
3 81 by Delgado-Torres et al. (2022) for the surface air temperature), area-dependent and lead-
4 82 time dependent.
5

6 83 We address the following questions:
7

- 8 84 - Are CMIP6 initialized prediction systems skilful at predicting summer monsoon
9 85 precipitation on interannual-to-decadal time scales?
10 86 - How model dependent is the skill at predicting summer monsoon precipitation?
11 87 - Can we identify the sources of skill?
12
13

14 88 The paper is organised as follows: section 2 describes the simulations and the
15 89 methodologies used. In section 3 we quantify skill at prediction monsoon precipitation for
16 90 the multi model mean and for each individual prediction system. Sources of skill are shown
17 91 in section 4. We discuss results in section 5 and section 6 concludes the main findings of the
18 92 study.
19
20

21 93
22

23 94
24
25
26
27
28
29
30
31
32
33
34
35
36
37
38
39
40
41
42
43
44
45
46
47
48
49
50
51
52
53
54
55
56
57
58
59
60

95 2. Methods and data

96 2.1 Data

97 We use hindcasts of 9 climate models from DCP Component A (Boer et al., 2016) (DCPPA
98 hereafter). These climate predictions are initialised from observationally constrained
99 datasets every year from 1960 to 2019 and 5 to 10 ensemble members are used depending
100 on the climate model (Table 1). We assume 5 to 10 ensemble members to be large enough
101 to allow considerably increased prediction skill of monsoon precipitation (Jain et al., 2019;
102 Monerie et al., 2021). DCPA simulations are initialised in November each year and last for 5
103 to 10 years after initialisation and are forced with historical external forcing.

104 We assess the impact of initialisation by comparing DCPA simulations to the uninitialized
105 CMIP6 historical simulations (Eyring et al., 2016; Table S1), using the same climate models.
106 These historical simulations begin in 1850 and last for ~150 years (1850-2014) and use the
107 same external forcings as the DCPA simulations. Prior to analysis, observations and
108 simulations are first interpolated onto a common 1° horizontal grid.

109 We assess skill at predicting precipitation using the data of the Climate Research Unit (CRU;
110 Harris et al. 2014), available from 1901 to present. Skill at predicting surface air temperature
111 is quantified using the NCEP reanalysis (Kanamitsu et al., 2002), which is given on a 2.5° x
112 2.5° horizontal resolution and from 1948 to present.

113 2.2 Method

114 2.2.1 Assessing skill

115 Prediction skill is estimated using the Anomaly Correlation Coefficient (ACC) metric,
116 computed between observed and simulated time series. We assess skill at three lead times.
117 The one-year lead time allows determination of skill at predicting interannual variability in
118 summer monsoon precipitation and is months 14-17 (8-11) for the southern (northern)
119 hemisphere in DJFM (JJAS). Years 2-5 and years 6-9 are 4 years averaged between year 2 to
120 5 and 6 to 9, respectively, and documents predictability of the summer monsoon
121 precipitation on longer time scales. Prediction skill is assessed over the period 1960-2020.

122 We estimate the significance of the ACC by randomly resampling time series of the
123 ensemble means. We use a 5-year block bootstrap to conserve low-frequency variability in
124 precipitation and temperature using 5000 permutations in a Monte Carlo framework. The
125 ACC values are judged significant at the $p < 0.05$ level if the correlations are stronger than
126 97.5% of the randomly obtained correlation values, using a two-sided test.

127 We acknowledge that ACC scores are sensitive to the existence of linear trends (*e.g.*, in
128 precipitation, Figure S1). However, we note that removing a linear trend can artificially
129 improve skill (Figure S2). Therefore, we document the skill at predicting the total summer
130 monsoon variability (internal variability + variability induced by the externally forced
131 response).

132 2.2.2 Drift correction

DCPPA simulations are initialised from observationally constrained datasets, but then drift away to reach their own model's climatology. The drift can result in fast and large changes in temperature and precipitation (Hermanson et al., 2018). Hence, we remove the lead-time-dependent drift following the World Climate Research Programme recommendations (ICPO, 2011) (see Drift Correction in the Supplementary Material) prior to displaying simulated time series. Note that removing the drift does not impact skill as defined by the ACC.

2.2.3 Persistence

The n -year persistence is computed based on the observed values in the n years prior to the start date. We computed a 1-year and a 4-year persistence.

2.2.4 Defining ensembles

We define ensembles to explore the spread in model skill and to understand sources of prediction skill for summer monsoon precipitation.

2.2.4.1 Ensemble mean (ENSM and HIST)

We assess the ability of DCPA simulations to predict monsoon precipitation by defining the ensemble mean across models and ensemble members, hereafter called ENSM, as:

$$\bar{P}(j) = \frac{1}{m} \sum_{i=1}^m P_i^j,$$

with P precipitation of all m ensemble members i and for each start date j , and \bar{P} precipitation averaged across all ensemble members and start date. m is the total number of ensemble members across all models.

HIST is defined in the same way as ENSM but using the uninitialized simulations. Uninitialized ensemble members simulate internal climate variability, but ensemble members would not be expected to be in-phase and the ensemble mean is an estimate of the forced response to external drivers (e.g., Deser et al. 2012). Therefore, the comparison of ENSM and HIST allows for an exploration of the importance of initialisation for the prediction skill.

2.2.4.2 Best Model (BEST)

The prediction system that performs best is selected, according to the ACC values, with the BEST ensemble consisting of only one individual model, for each monsoon domain and each lead-time.

2.2.4.3 A subset of models (SUBSET and WORST SUBSET)

The SUBSET approach follows the ENSM approach, computing the ensemble mean with only the three prediction systems that have the highest ACC values over a given monsoon domain and for a given lead time. The composition of the SUBSET ensemble is, thus, monsoon domain and lead time dependent.

1
2
3 168 The WORST SUBSET is defined in the same way as SUBSET but selecting the three prediction
4 169 models that have the lowest ACC values. We expect a comparison of SUBSET against WORST
5 170 SUBSET and ENSM to provide information on sources of prediction skill. Finally, the effect of
6 171 initialisation is here estimated by comparing SUBSET with HIST SUBSET, which is composed
7 172 of the same models as SUBSET but using historical uninitialized simulations only.

10 173 **2.2 Monsoon domains**

11
12 174 Monsoon domains are defined where the difference between May to September (MJJAS)
13 175 and November to March (NDJFM) precipitation exceeds 2.5 mm.d^{-1} (Wang et al., 2011) in
14 176 observations (GPCC; Schneider et al. 2014). We only consider precipitation that falls within
15 177 the tropical latitudes $[30^{\circ}\text{S}-30^{\circ}\text{N}]$ and over land. Monsoon domains are shown in Figure 1
16 178 and are named NAM (Northern America), NAF (Northern Africa), SAS (South Asia), EAS (East
17 179 Asia), SAM (Southern America), SAF (Southern Africa) and AUS (Australia), following the
18 180 literature (e.g., Kitoh et al. 2013). We assess skill at predicting summer monsoon
19 181 precipitation, in JJAS for the NAM, NAF, SAS and EAS monsoon domains and in DJFM for the
20 182 SAM, SAF and AUS monsoon domains. In addition, we averaged monsoon precipitation of all
21 183 domains in the northern (NHM) and southern (SHM) Hemispheres.

26 184 **2.3 The Interdecadal Pacific Oscillation**

27
28 185 We define the Interdecadal Pacific Oscillation (IPO) as the difference between the central-
29 186 eastern Pacific $[150^{\circ}\text{E}-150^{\circ}\text{W}; 10^{\circ}\text{S}-10^{\circ}\text{N}]$ and the tropical central-eastern Pacific $[170^{\circ}\text{W}-$
30 187 $90^{\circ}\text{W}; 25^{\circ}\text{N}-45^{\circ}\text{N}]$ after Huang et al. (2020), using surface air temperature. According to
31 188 Huang et al. (2020), this index gives similar results that the tripole index of Henley et al.
32 189 (2015).

33
34
35 190

36
37
38 191

3. DCPPA prediction skill

3.1 Quantifying DCPPA ensemble-mean prediction skill

We assess prediction skill of ENSM for summer monsoon precipitation at each grid point, and when averaged over each monsoon domain.

We find significant skill in predicting summer monsoon precipitation in ENSM, but the skill appears to increase with lead time. Figure 1a shows that skill at predicting precipitation at the 1-year forecast lead time is relatively low over much of the globe, although there are regions with statistically significant prediction skill. For example, over the tropics, prediction skill is significant over northern South America, Argentina, and the western Sahel. Nevertheless, relative to the 1-year predictions, we find an increase in skill for the 2-5 and 6-9 forecast lead times. This increase in skill stands out over the Sahel, western India and Southeast Asia, and northern South America (Figure 1b and Figure 1c).

Figure 2 shows the skill at predicting summer monsoon precipitation when averaged over all monsoon domains. At the 1-year forecast lead time, ENSM is skilful at predicting NAM and AUS precipitation, as well as the hemisphere-wide quantities (NHM and SHM) (Figure 2a). However, there is no significant skill over the NAF, SAS, EAS, SAM and SAF monsoon domains. For the 2-5 and 6-9-year forecast lead times, skill remains statistically significant for NHM, SHM, and NAM precipitation (Figure 2b and Figure 2c) and increases substantially for NAF and SAM precipitation. In contrast, ENSM does not show significant skill for the SAS, EAS and SAF monsoon domains for any lead-time. Results show higher skill for ENSM than for the CMIP5 decadal prediction systems (Bellucci et al. 2015).

We assess the sources of model skill at predicting summer monsoon precipitation variability compared with persistence forecasts and with uninitialized simulations. Figure 2 shows that ENSM prediction skill generally exceeds persistence, implying that the skill does not only depend on the inertia of the climate system. We note, however, that persistence is more skilful than ENSM for the 1-year and 2-5-year forecast lead times for NAF summer monsoon precipitation (Figure 2a and Figure 2b). The effect of initialisation (defined as the difference between initialised and uninitialized hindcasts) only emerges for a limited number of monsoon domains, especially at the longer lead times (*e.g.*, 6-9 years), indicating that changes in external forcing are an important source of prediction skill on these time scales.

3.2 Understanding the range of prediction skill

So far, we have only explored the multi-model mean skill. But modelling systems will likely exhibit different levels of skill. Figure 2 also shows the range of skill for each model in the DCPPA ensemble and there is a significant diversity of model skill for all lead times (purple vertical lines). There is a consensus for some monsoon domains and lead-times, with all models exhibiting positive skill (*e.g.*, NAM summer monsoon precipitation for the 1-year forecast lead-time and NAF summer monsoon precipitation for the 2-5 and 6-9 forecast lead-times). However, there is more diversity in prediction skill for the SAS and EAS domains, with individual models performing much better or lesser than ENSM (Figure 2b and Figure 2c), as also shown with seasonal hindcasts (Jain et al., 2019; Mishra et al., 2018). Skill scores for each model and monsoon domain are shown in Figure S3 and Figure S4.

4. Sources of prediction skill

We explore the source of skill by selecting models according to their prediction skill. As expected, the BEST and SUBSET ensembles generally show improved skill relative to ENSM for all forecast lead time (Figure 3).

ACC value is around tripled in SUBSET (ACC=0.61) compared to ENSM (ACC=0.18) for EAS summer monsoon precipitation and the 2–5-year forecast lead time (Figure 3b and Table S2). ACC values is approximately quadrupled in SUBSET (ACC=0.40) relative to ENSM (ACC=0.09) for SAS summer monsoon precipitation and for the 6–9-year forecast lead time (Figure 3c and Table S3). This is a consequence of the large diversity in prediction skill over South and East Asia, with prediction systems exhibiting either high or low skill. Thus, skilful predictions can be obtained in the regions that ENSM is not skilful. We used another observational dataset (GPCC) and show that results are robust across observations (not shown).

4.1 Source of prediction skill for EAS summer monsoon precipitation

We focus on prediction of EAS summer monsoon precipitation for the 2–5-year forecast lead time, for which the SUBSET-ENSM difference in skill is the largest. The improved skill in SUBSET, relative to ENSM, is largely due to the multi-decadal variation in EAS summer monsoon precipitation. After applying a 7-year running mean to the 2-5-year forecasts we find the ACC is 0.70 in SUBSET but only 0.14 in ENSM. This is further confirmed using a 21-year running mean to only capture the slow variation of the EAS summer monsoon precipitation (Figure S5). In contrast, the difference in skill between SUBSET (ACC=0.18) and ENSM (ACC=0.07) is low when considering higher frequency variability (defined as the residual relative to the 7-year running mean). Figure 4a shows the smoothed time series in EAS summer monsoon precipitation. Although there is significant skill in SUBSET, both ENSM and SUBSET ensemble underestimate the observed variability. The difference between SUBSET and ENSM ensembles is that there is a long-lasting drying trend in ENSM while SUBSET simulates a small decrease in precipitation from 1960 to the 1980s and an increase in precipitation afterwards, hence better following the observation (Figure 4a). In contrast, the WORST SUBSET shows a strong drying trend. Therefore, the difference in trends appears to be key to understand the differences in monsoon precipitation skill.

There is a large effect of the externally forced response on the multi-annual variation in EAS summer monsoon precipitation, as evidenced by the high correlation coefficient between the uninitialized and initialised simulations ($r^*=0.94$ between ENSM and HIST; Figure 4a).

Hence, we hypothesise that the range in skill of the DCPA ensemble to be due to the differences in the response to external forcing. This is assessed by comparing maps of SUBSET-WORST SUBSET difference in skill (Figure 5a) to the HIST SUBSET-HIST WORST SUBSET difference in skill (Figure 5b). As the skill of uninitialized simulations is due to the response to the external forcing, the strong similarity between Figure 5a and Figure 5b confirms a strong role of the simulation of the externally forced response on the spread in prediction skill over EAS. These results have a strong societal importance because the

273 increase in skill is the highest over eastern China, a heavily populated region where
274 precipitation variability is high (Figure 5a).

275 **4.2 Sources of prediction skill for SAS summer monsoon precipitation**

276 We focus on prediction of SAS summer monsoon precipitation for the 6–9-year forecast
277 lead time, for which the SUBSET-ENSM difference in skill is the greatest. As for EAS summer
278 monsoon precipitation, the externally forced response has strong effects on the long-term
279 variation in simulated SAS summer monsoon, as shown by the high correlation coefficient
280 between uninitialized and initialised simulations ($r^*=0.98$ between ENSM and HIST; Figure
281 4b). The spread in SAS summer monsoon prediction skill is also associated with the ability of
282 prediction systems to simulate the multi-decadal variation in SAS summer monsoon
283 precipitation. This is evidenced by the absence of pre-1990 drying in WORST SUBSET, while
284 SUBSET shows a multi-decadal variation in SAS summer monsoon precipitation, in better
285 agreement with the observations (Figure 4b).

286 An effect of the response to external forcing on the spread of South Asian summer monsoon
287 prediction skill is confirmed by the similarity between patterns of difference in prediction
288 skill (SUBSET-WORST SUBSET; Figure 5c, and HIST SUBSET- HIST WORST SUBSET; Figure 5d).
289 However, the response to externally forced response does not fully explain the SUBSET-
290 WORST SUBSET difference in skill. We thus also expect other drivers of South Asian summer
291 monsoon precipitation variability to contribute to the spread in SAS summer monsoon
292 precipitation skill.

293 The multi-decadal variability in South Asian precipitation has been linked to the interdecadal
294 variability of the Pacific Ocean (IPO) (Huang et al., 2020; Zhang et al., 2018). We show a
295 strong relationship between skill at predicting the IPO and that of the SAS summer monsoon
296 precipitation at the 6–9-year forecast lead time (Figure 6b; $r=0.88$). The spread at predicting
297 the IPO thus also contribute to the spread at prediction the SAS summer monsoon
298 precipitation. We performed the same analysis with the uninitialized simulations and show
299 that the result of Figure 6b is due to initialisation ($r=0.01$ with the uninitialized simulations),
300 and thus to the simulation of internal climate variability and to the correction of an incorrect
301 forced response.

302 **5 Discussion**

303 Although we show improved skill over EAS and SAS summer monsoon precipitation in
304 SUBSET, which we attribute to the impact of external forcing and to the simulation of the
305 IPO, the exact mechanisms that explain the higher skill are unclear. For example, we
306 explored mechanisms focusing on known drivers of the monsoon circulation, such as the
307 large-scale gradients in surface air temperature and of surface air temperature over the
308 oceans. However, differences in skill at predicting surface air temperature between the
309 SUBSET and ENSM ensembles are low (Figure S6 and Figure S7). Further work could focus on
310 understanding differences in atmospheric circulation, and regional changes between
311 SUBSET and ENSM. We also acknowledge that different estimations of the internal
312 components of the IPO could lead to different conclusions and future work could be
313 devoted to understanding what leads to better prediction skill of the IPO and its role for

1
2
3 314 predicting summer monsoon precipitation at multi-annual forecast lead times. In addition,
4 315 the results are expected to be sensitive to the estimate of the IPO (*e.g.*, (Henley et al., 2015;
5 316 Parker et al., 2007) and to the use of different observations/reanalysis. However, we show
6 317 that skill at predicting South Asian summer monsoon precipitation is sensitive to the skill at
7 318 predicting the Pacific Ocean SSTs for the 6-9-year forecast lead-time.

10 319 We explored further the role of the IPO indices on summer monsoon prediction skill,
11 320 correcting IPO indices and effects on summer monsoon precipitation, using observations.
12 321 We show that an improved prediction skill for the IPO leads to a better prediction skill for
13 322 the SAS summer monsoon precipitation (Figure S8 and text in the supplementary material).
14 323 Better predicting the IPO can allow improved prediction skill over South Asia. In addition to
15 324 the IPO, we found a moderate relationship between skill at predicting North Atlantic
16 325 temperature and SAS summer monsoon precipitation ($r=0.35$) for the 6-9- year forecast
17 326 lead-time. In contrast, prediction skill of the IPO has no effects on prediction skill for EAS
18 327 summer monsoon precipitation (Figure 6a; $r=-0.18$) and we found no relationship between
19 328 prediction of the North Atlantic, Indian Ocean, and equatorial Pacific Ocean temperature on
20 329 prediction skill of EAS summer monsoon precipitation skill (not shown) for the 2-5- year
21 330 forecast lead-time.

27 331 We acknowledge here that we do not suggest the full skill of the prediction systems to arise
28 332 only due to the externally forced response. Instead, we suggest that differences in skill in
29 333 initialised predictions are partly due to differences in the simulation of the externally forced
30 334 response. These differences in skill could be due to model biases. However, we found no
31 335 relationships between biases in seasonal mean precipitation (or variability) and prediction
32 336 skill, when using monsoon domain averages (not shown). Yet, further work might identify
33 337 the importance of model biases for prediction skill. A focus could be given to the biases in
34 338 simulation of the mean state tropical SSTs (*e.g.*, Turner et al. 2005). We also highlight that
35 339 an increased number of models could allow increasing robustness of the results.

39 340 **6 Conclusions**

41 341 We quantify the ability of CMIP6 initialized decadal prediction systems (Boer et al. 2016) to
42 342 predict summer monsoon precipitation in a global monsoon framework and focus on three
43 343 forecast lead times (1 year, 2-5 years, and 6-9 years). Overall, skill is low for the forecast 1-
44 344 year lead time but increases for the 2-5- and 6-9-year horizons. Furthermore, the skill is
45 345 model dependent, monsoon-domain dependent and lead-time dependent.

48 346 We explore sources of skill for predicting summer monsoon precipitation. In particular, the
49 347 impact of initialisation is rather small when focusing on the 2-5 and 6-9 forecast lead times.
50 348 Therefore, the results highlight the importance of the externally forced response for
51 349 providing skill at predicting summer monsoon precipitation. By selecting models, based on
52 350 their prediction skill, we suggest that differences in simulating the externally forced
53 351 response between models explains a large proportion of the diversity skill of the CMIP6
54 352 model ensemble, over South and East Asia.

58 353 Nevertheless, differences in skill at predicting the Interdecadal Pacific Oscillation (IPO) also
59 354 contributes to differences in skill between models for predictions of the South Asian

1
2
3 355 summer monsoon precipitation at the 6-9-year forecast lead time. We show that
4 356 initialisation and improved prediction of the Pacific SSTs is important for prediction of South
5 357 Asian summer monsoon precipitation, but it is unclear if this is due to improved prediction
6 358 of internal variability, a correction of an incorrect forced response or mean state. Besides,
7 359 we acknowledge that skill at predicting the IPO can be a manifestation of an effect of the
8 360 externally forced response on temperature over the Pacific Ocean. Therefore, improving our
9 361 understanding of the differences between how models simulate the effects of external
10 362 forcing and of the Interdecadal Pacific Oscillation on South and East Asian summer monsoon
11 363 precipitation could be an important avenue for improving prediction skill on a multi-annual
12 364 time scale. The mechanism (*e.g.*, anomalies in atmospheric circulation, in temperature
13 365 gradients) that explains model skill diversity remains unclear. Further work is needed,
14 366 focusing on, for instance, the atmosphere dynamics or model biases.

15 367 We do not argue here that selecting models based on their prediction skill should be used
16 368 for predicting the future evolution of the East and South Asian summer monsoon
17 369 precipitation up to ten years ahead. A reason for that is that prediction skill depends on the
18 370 period used as reference (Figure S9) and the ensembles might thus not provide the best
19 371 prediction for the coming decade.

20 372

21 373 **Acknowledgements.**

22 374
23 375 JR was funded by NERC via the ACSIS (NE/N018001/1) and CANARI (NE/W004984/1)
24 376 programs, and the WISHBONE (NE/T013516/1) project. CDN was supported by PDI/MS
25 377 (Programme Doctoral International: Modélisation des Systèmes Complexes), the scholarship
26 378 of SCAC (Service de Coopération et d'Action Culturelle), the ERASUMUS+ programme
27 379 through action KA107, and the Laboratoire Mixte International ECLAIRS2 (IRD), the UCM
28 380 XVII call for cooperation and sustainable development. AGT was funded via the National
29 381 Centre for Atmospheric Science through the NERC National Capability International
30 382 Programme Award (NE/X006263/1).

31 383
32 384 We acknowledge the World Climate Research Programme's Working Group on Coupled
33 385 Modelling, which is responsible for CMIP, and we thank the climate modelling groups for
34 386 producing and making available their model output. For CMIP the U.S. Department of
35 387 Energy's Program for Climate Model Diagnosis and Intercomparison provides coordinating
36 388 support and led development of software infrastructure in partnership with the Global
37 389 Organization for Earth System Science Portals. We also thank the two anonymous reviewers
38 390 for their comments and suggestions.

39 391

40 392

41 393 **Data availability statement**

42 394 CMIP6 GCM output is available at <https://esgf-node.llnl.gov/search/cmip6/>. DOIs/URLs for
43 395 the historical simulations are <https://doi.org/10.22033/ESGF/CMIP6.3610>,

1
2
3 396 <https://doi.org/10.22033/ESGF/CMIP6.3825>, <https://doi.org/10.22033/ESGF/CMIP6.4700>,
4 397 <https://doi.org/10.22033/ESGF/CMIP6.6112>, <https://doi.org/10.22033/ESGF/CMIP6.5195>,
5 398 <https://doi.org/10.22033/ESGF/CMIP6.5603>, <https://doi.org/10.22033/ESGF/CMIP6.6594>,
6 399 <https://doi.org/10.22033/ESGF/CMIP6.6842>, <https://doi.org/10.22033/ESGF/CMIP6.10894>,
7 400 respectively for CanESM5, CMCC-CM2-SR5, EcEARTH3, HadGEM3-GC31-MM, IPSL-CM6A-LR,
8 401 MIROC6, MPI-ESM1-2-HR, MRI-ESM2-0 and NorCPM1. DOIs/URL for the hindcasts are
9 402 <https://doi.org/10.22033/ESGF/CMIP6.3557>, <https://www.wdc->
10 403 [climate.de/ui/entry?acronym=C6_4368435](https://doi.org/10.22033/ESGF/CMIP6.4553), <https://doi.org/10.22033/ESGF/CMIP6.4553>,
11 404 <https://doi.org/10.22033/ESGF/CMIP6.5892>, <https://doi.org/10.22033/ESGF/CMIP6.5137>,
12 405 <https://doi.org/10.22033/ESGF/CMIP6.890>, <https://doi.org/10.22033/ESGF/CMIP6.768>,
13 406 <https://doi.org/10.22033/ESGF/CMIP6.630> and
14 407 <https://doi.org/10.22033/ESGF/CMIP6.10865>, respectively for CanESM5, CMCC-CM2-SR5,
15 408 EcEARTH3, HadGEM3-GC31-MM, IPSL-CM6A-LR, MIROC6, MPI-ESM1-2-HR, MRI-ESM2-0 and
16 409 NorCPM1. NCEP temperature data are provided by the NOAA/OAR/ESRL PSL, Boulder,
17 410 Colorado, USA, from their website at
18 411 <https://downloads.psl.noaa.gov/Datasets/ncep.reanalysis/Monthlies/pressure/>. CRU
19 412 Precipitation is provided by the Climate Research Unit, from the website at
20 413 https://crudata.uea.ac.uk/cru/data/hrg/cru_ts_4.03/cruts.1905011326.v4.03/pre/.
21 414
22 415
23 416
24 417
25 418
26 419
27
28
29
30
31
32
33
34
35
36
37
38
39
40
41
42
43
44
45
46
47
48
49
50
51
52
53
54
55
56
57
58
59
60

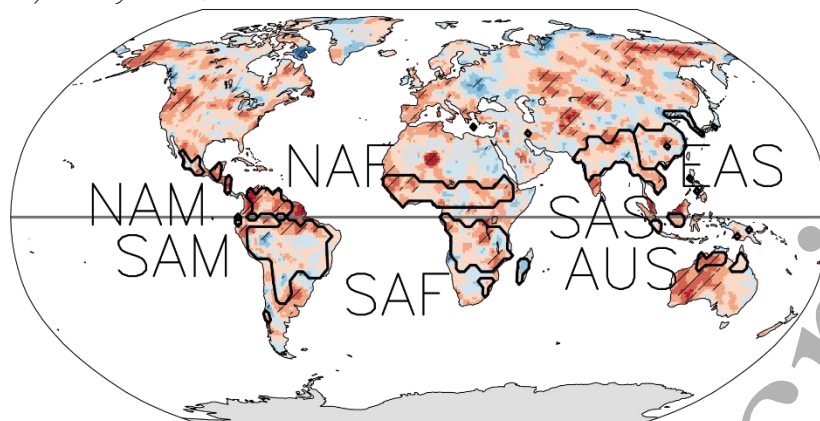
| Models | Institutions | No. of ensemble members | Length of the integrations (years) | Horizontal resolution (lat x lon) | References |
|-----------------|--|-------------------------|------------------------------------|-----------------------------------|--------------------------|
| CanESM5 | Canadian Center for Climate Modeling and Analysis, Canada | 10 | 10 | 64 x 128 | (Swart et al., 2019) |
| CMCC-CM2-SR5 | Fondazione Centro Euro-Mediterraneo sui Cambiamenti Climatici. Italy | 6 | 10 | 192 x 288 | (Cherchi et al., 2019) |
| EcEarth3 | EC-Earth-Consortium | 10 | 10 | 256 x 512 | (Wyser et al., 2020) |
| HadGEM3-GC31-MM | Met Office Hadley Centre, United Kingdom | 10 | 10 | 324 x 432 | (Kuhlbrodt et al., 2018) |
| IPSL-CM6A-LR | Institut Pierre Simon Laplace, France | 10 | 10 | 144 x 143 | (Boucher et al., 2020) |
| MIROC6 | Japanese modeling community, Japan | 10 | 10 | 128 x 256 | (Tatebe et al., 2019) |
| MPI-ESM1-2-HR | Deutsches Klimarechenzentrum, Germany | 5 | 10 | 192 x 384 | (Mauritsen et al., 2019) |
| MRI-ESM2-0 | Meteorological Research Institute, Japan | 10 | 5 | 160 x 320 | (Yukimoto et al., 2019) |
| NorCPM1 | NorESM Climate modeling Consortium | 10 | 10 | 96 x 144 | (Bethke et al., 2021) |

420 Table 1: List of DCPPA prediction systems and number of simulations used in the study

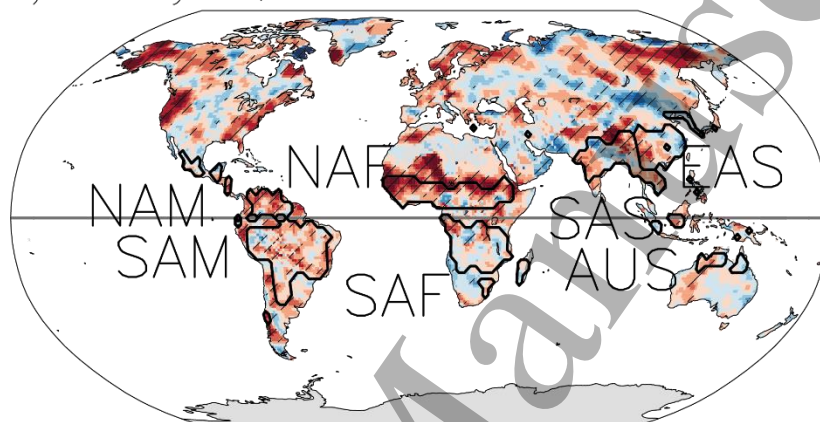
421

1
2
3
4
5
6
7
8
9
10
11
12
13
14
15
16
17
18
19
20
21
22
23
24
25
26
27
28
29
30
31
32
33
34
35
36
37
38
39
40
41
42
43
44
45
46
47
48
49
50
51
52
53
54
55
56
57
58
59
60

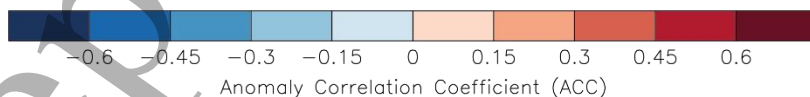
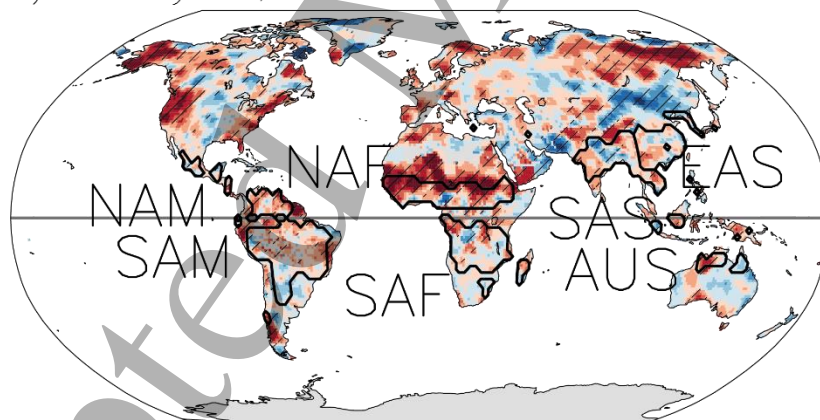
a) 1 year; ENSM



b) 2–5 year; ENSM

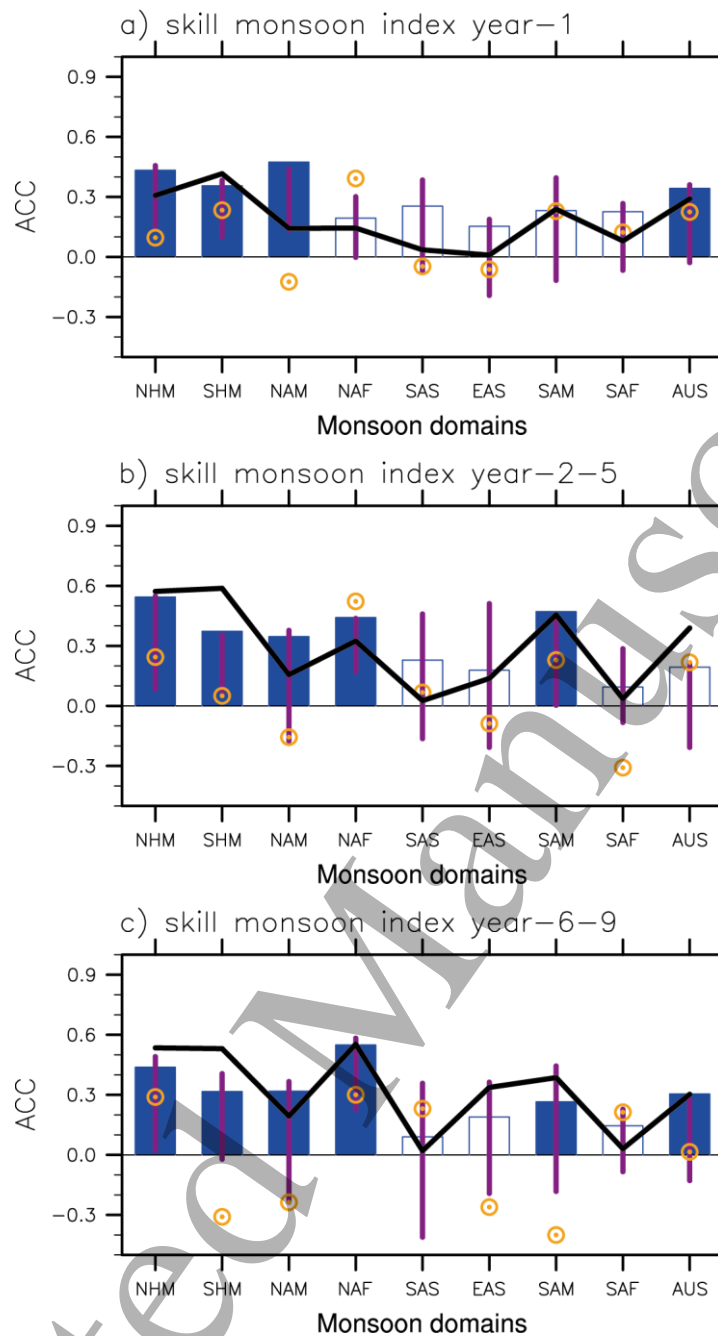


c) 6–9 year; ENSM



422

423 **Figure 1.** Anomaly correlation coefficient skill score for predictions of precipitation in ENSM at the
 424 (a) 1, (b) 2–5 and (c) 6–9-year forecast lead times, relative to CRU. ACC values are shown for JJAS
 425 (DJFM) in the northern (southern) hemisphere. Stippling indicates that ACC is significantly different
 426 to zero according to a Monte-Carlo procedure with 5000 permutations and a 95% confidence level.
 427 Black contours show the monsoon domains.



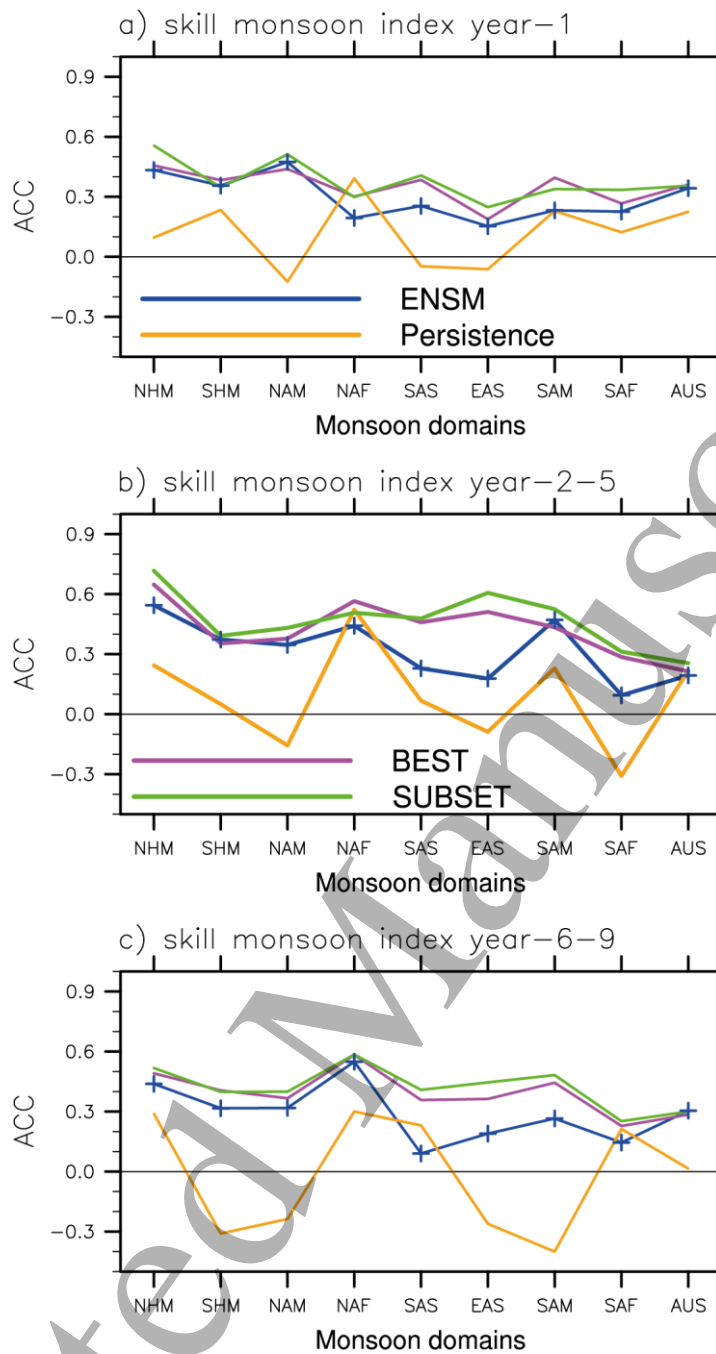
428

429 **Figure 2:** Anomaly correlation coefficient skill score for predictions of summer monsoon
 430 precipitation averaged over each monsoon domain and for the northern hemisphere (NHM) and the
 431 southern hemisphere (SHM). Results are given for ENSM (bars), uninitialized simulations (black line),
 432 and persistence (orange circles), and for the (a) 1-year, (b) 2-5 year, and (c) 6-9-year forecast lead
 433 times. The magenta vertical line shows the range in DCPA prediction skill, defined between the
 434 lowest and highest skill and from each prediction system. A solid blue bar indicates that ACC is
 435 significantly different to zero according to a Monte-Carlo procedure with 5000 permutations and a
 436 95% confidence level.

437

438

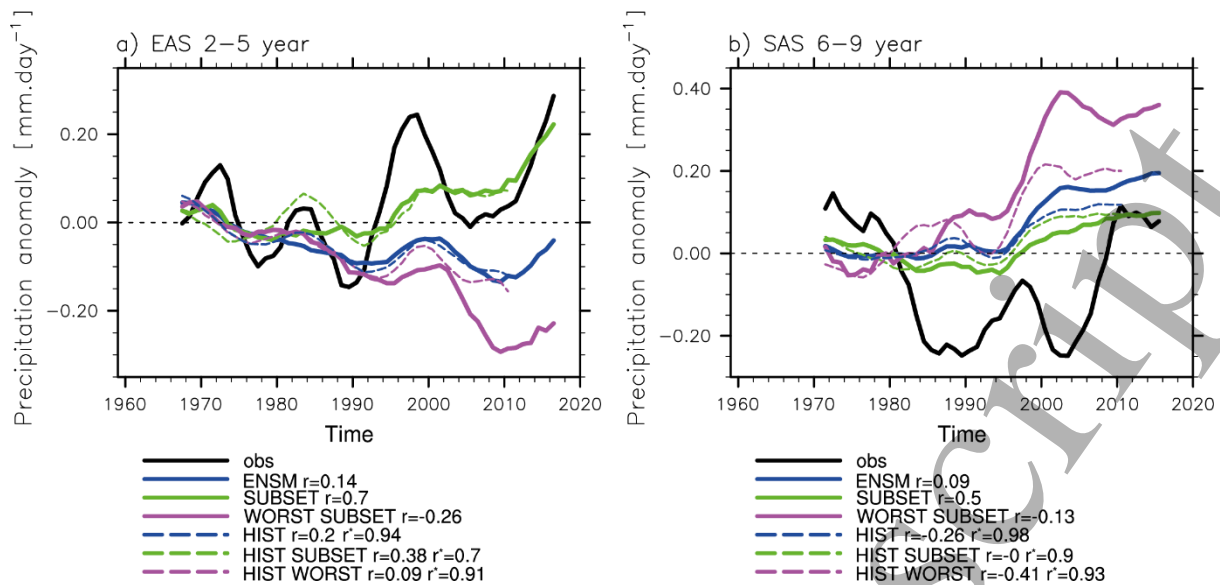
439



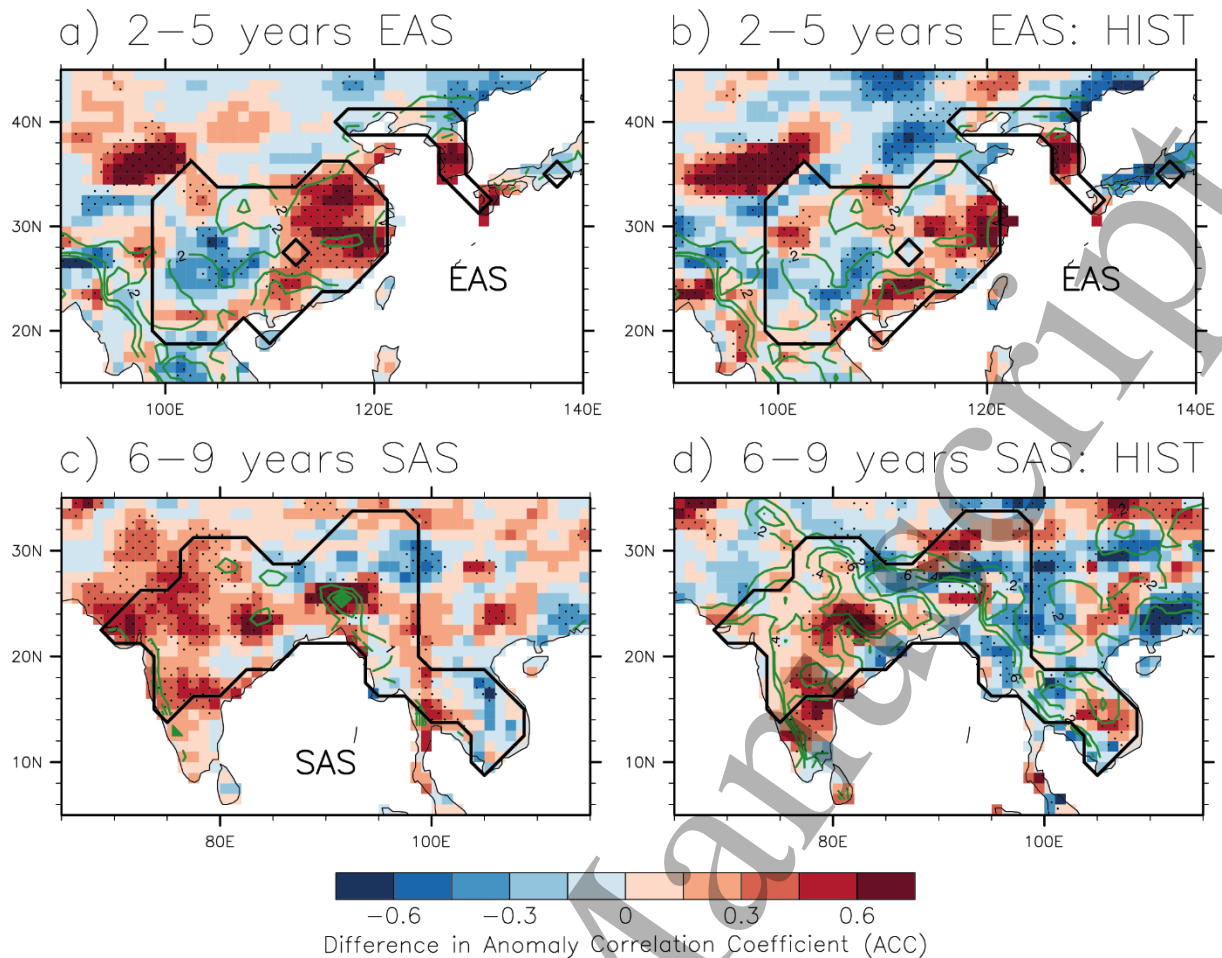
440

441 **Figure 3:** Anomaly correlation coefficient skill score for predictions of summer monsoon
 442 precipitation averaged over the northern hemisphere (NHM), the southern hemisphere (SHM) and
 443 each monsoon domain. Results are given for ENSM (dark blue), persistence (orange), BEST
 444 (magenta), and SUBSET (light green). Results are given for the (a) 1-year, (b) 2-5 year, and (c) 6-9-
 445 year forecast lead times.

446



447
448 **Figure 4:** Precipitation anomalies in (a) EAS and (b) SAS summer monsoons, for the 2-5- and 6-9-year
449 forecast lead times, respectively. Observations (CRU) are shown in black, ENSM in blue, SUBSET in
450 green, WORST SUBSET in magenta, and HIST with discontinuous black line. Anomalies are computed
451 relative to the 1961-1981 period. The high frequency variability is removed using a 7-year running
452 average after computing the 2-5 and 6-9 averages. The r number indicates the ACC value, computed
453 between each ensemble and observations, the r^* number indicates the correlation coefficient
454 between initialized and uninitialized simulations.



459

460 **Figure 5:** SUBSET minus WORST SUBSET difference in anomaly correlation coefficient skill score for
 461 predictions of precipitation over (a) East Asia for the 2-5-year forecast lead time, (c) South Asia for
 462 the 6-9-year forecast lead time. Skill at predicting precipitation is computed in comparison to CRU.
 463 Green contours indicate the precipitation variance, in $\text{mm}^2 \cdot \text{d}^{-2}$. (b) and (d), as in (a) and (c) but for
 464 the HIST SUBSET-HIST WORST SUBSET difference in anomaly correlation coefficient skill score for
 465 precipitation. Stippling indicates that the difference in ACC is significantly different to zero according
 466 to a Monte-Carlo procedure, resampling both BEST and ENSM and computing difference in ACC
 467 values. We use 5000 permutations and a 95% confidence level. The same number of ensemble
 468 members are used for the ensembles of initialised and uninitialized simulations (19 ensemble
 469 members for HIST SUBSET and 26 ensemble members for WORST SUBSET for EAS summer monsoon
 470 precipitation; 30 ensemble members for HIST SUBSET and 15 ensemble members for WORST SUBSET
 471 and for the SAS summer monsoon precipitation.)

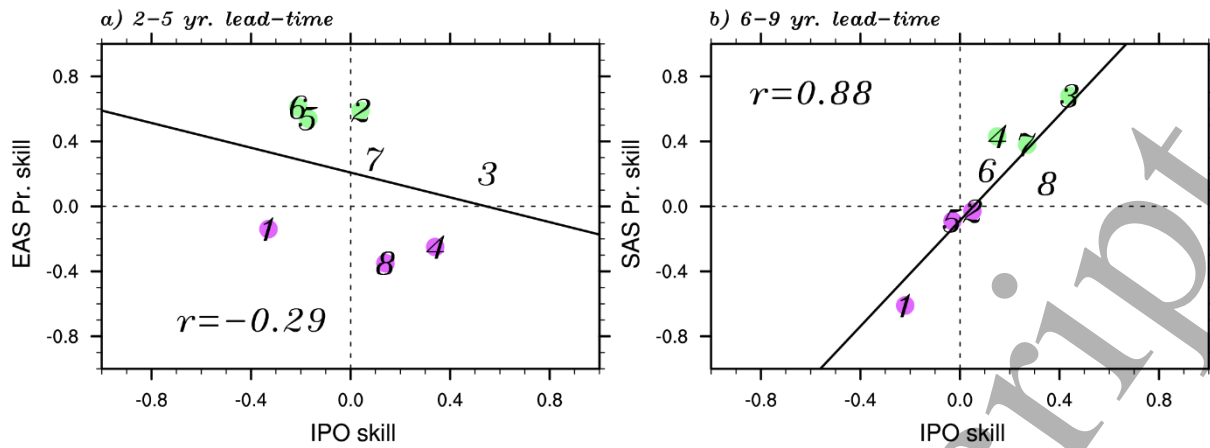
472

473

474

475

476



477

478 **Figure 6:** Anomaly correlation coefficient skill score for predictions of IPO index and (a) EAS and (b)
 479 SAS summer monsoon precipitation for each prediction system (1-CMCC-CM2-SR5; 2-HadGEM3-
 480 GC31-MM; 3-IPSL-CM6A-LR; 4-MIROC6; 5-MPI-ESM1-2-HR; 6-CanESM5; 7-EcEarth3; 8-NorCPM1)
 481 and the 2-5- and 6-9-year forecast lead times, respectively. A 7-year running mean was applied to
 482 both precipitation and IPO time series before to compute anomaly correlation coefficients. SUBSET
 483 (WORST SUBSET) models are shown with a green (magenta) circle.

484

1
2
3 485 **References**
4

- 5 486 Bellucci, A., Haarsma, R., Gualdi, S., Athanasiadis, P. J., Caian, M., Cassou, C., Fernandez, E., Germe,
6 487 A., Jungclaus, J., Kröger, J., Matei, D., Müller, W., Pohlmann, H., Salas y Melia, D., Sanchez, E.,
7 488 Smith, D., Terray, L., Wyser, K., & Yang, S. (2015). An assessment of a multi-model ensemble of
8 489 decadal climate predictions. *Climate Dynamics*, 44(9–10), 2787–2806.
9 490 <https://doi.org/10.1007/s00382-014-2164-y>
- 11 491 Beraki, A. F., DeWitt, D. G., Landman, W. A., & Olivier, C. (2013). Dynamical Seasonal Climate
12 492 Prediction Using an Ocean–Atmosphere Coupled Climate Model Developed in Partnership
13 493 between South Africa and the IRI. *Journal of Climate*, 27(4), 1719–1741.
14 494 <https://doi.org/10.1175/JCLI-D-13-00275.1>
- 16 495 Bethke, I., Wang, Y., Counillon, F., Keenlyside, N., Kimmritz, M., Fransner, F., Samuelsen, A.,
17 496 Langehaug, H., Svendsen, L., Chiu, P.-G., Passos, L., Bentsen, M., Guo, C., Gupta, A., Tjiputra, J.,
18 497 Kirkevåg, A., Olivié, D., Seland, Ø., Solsvik Vågane, J., ... Eldevik, T. (2021). NorCPM1 and its
19 498 contribution to CMIP6 DCP. *Geoscientific Model Development*, 14(11), 7073–7116.
20 499 <https://doi.org/10.5194/gmd-14-7073-2021>
- 23 500 Boer, G. J., Smith, D. M., Cassou, C., Doblas-Reyes, F., Danabasoglu, G., Kirtman, B., Kushnir, Y.,
24 501 Kimoto, M., Meehl, G. A., Msadek, R., Mueller, W. A., Taylor, K. E., Zwiers, F., Rixen, M.,
25 502 Ruprich-Robert, Y., & Eade, R. (2016). The Decadal Climate Prediction Project (DCPP)
26 503 contribution to CMIP6. *Geoscientific Model Development*, 9(10), 3751–3777.
27 504 <https://doi.org/10.5194/gmd-9-3751-2016>
- 29 505 Boucher, O., Servonnat, J., Albright, A. L., Aumont, O., Balkanski, Y., Bastrikov, V., Bekki, S., Bonnet,
30 506 R., Bony, S., Bopp, L., Braconnot, P., Brockmann, P., Cadule, P., Caubel, A., Cheruy, F., Codron,
31 507 F., Cozic, A., Cugnet, D., D’Andrea, F., ... Vuichard, N. (2020). Presentation and Evaluation of the
32 508 IPSL-CM6A-LR Climate Model. *Journal of Advances in Modeling Earth Systems*, 12(7),
33 509 e2019MS002010. <https://doi.org/10.1029/2019MS002010>
- 35 510 Charney, J. G., & Shukla, J. (1981). *Predictability of monsoons*. *Monsoon Dynamics*, J. Lighthill and RP
36 511 Pearce, Eds. Cambridge University Press.
- 38 512 Cherchi, A., Fogli, P. G., Lovato, T., Peano, D., Iovino, D., Gualdi, S., Masina, S., Scoccimarro, E.,
39 513 Materia, S., Bellucci, A., & Navarra, A. (2019). Global Mean Climate and Main Patterns of
40 514 Variability in the CMCC-CM2 Coupled Model. *Journal of Advances in Modeling Earth Systems*,
41 515 11(1), 185–209. <https://doi.org/10.1029/2018MS001369>
- 43 516 Chevuturi, A., Turner, A. G., Johnson, S., Weisheimer, A., Shonk, J. K. P., Stockdale, T. N., & Senan, R.
44 517 (2021). Forecast skill of the Indian monsoon and its onset in the ECMWF seasonal forecasting
45 518 system 5 (SEAS5). *Climate Dynamics*, 56(9), 2941–2957. [https://doi.org/10.1007/s00382-020-](https://doi.org/10.1007/s00382-020-05624-5)
46 519 [05624-5](https://doi.org/10.1007/s00382-020-05624-5)
- 48 520 Delgado-Torres, C., Donat, M. G., Gonzalez-Reviriego, N., Caron, L.-P., Athanasiadis, P. J.,
49 521 Bretonnière, P.-A., Dunstone, N. J., Ho, A.-C., Nicoli, D., Pankatz, K., Paxian, A., Pérez-Zanón, N.,
50 522 Cabré, M. S., Solaraju-Murali, B., Soret, A., & Doblas-Reyes, F. J. (2022). Multi-Model Forecast
51 523 Quality Assessment of CMIP6 Decadal Predictions. *Journal of Climate*, 35(13), 4363–4382.
52 524 <https://doi.org/10.1175/JCLI-D-21-0811.1>
- 54 525 Deser, C., Phillips, A., Bourdette, V., & Teng, H. (2012). Uncertainty in climate change projections: the
55 526 role of internal variability. *Climate Dynamics*, 38(3), 527–546. [https://doi.org/10.1007/s00382-](https://doi.org/10.1007/s00382-010-0977-x)
56 527 [010-0977-x](https://doi.org/10.1007/s00382-010-0977-x)
- 58 528 Dunstone, N., Smith, D., Yeager, S., Danabasoglu, G., Monerie, P.-A., Hermanson, L., Eade, R., Ineson,
59 529 S., Robson, J. I., & Scaife, A. A. (2020). Skilful interannual climate prediction from two large

- 1
2
3 530 initialised model ensembles. *Environmental Research Letters*.
4
5 531 Eyring, V., Bony, S., Meehl, G. A., Senior, C. A., Stevens, B., Stouffer, R. J., & Taylor, K. E. (2016).
6 532 Overview of the Coupled Model Intercomparison Project Phase 6 (CMIP6) experimental design
7 533 and organization. *Geoscientific Model Development*, 9(5), 1937–1958.
8 534 <https://doi.org/10.5194/gmd-9-1937-2016>
9
10 535 Gaetani, M., & Mohino, E. (2013). Decadal Prediction of the Sahelian Precipitation in CMIP5
11 536 Simulations. *Journal of Climate*, 26(19), 7708–7719. <https://doi.org/10.1175/JCLI-D-12-00635.1>
12
13 537 García-Serrano, J., Guemas, V., & Doblas-Reyes, F. J. (2015). Added-value from initialization in
14 538 predictions of Atlantic multi-decadal variability. *Climate Dynamics*, 44(9–10), 2539–2555.
15 539 <https://doi.org/10.1007/s00382-014-2370-7>
16
17 540 Guemas, V., Corti, S., García-Serrano, J., Doblas-Reyes, F. J., Balmaseda, M., Magnusson, L., Guemas,
18 541 V., Corti, S., García-Serrano, J., Doblas-Reyes, F. J., Balmaseda, M., & Magnusson, L. (2013). The
19 542 Indian Ocean: The Region of Highest Skill Worldwide in Decadal Climate Prediction*. *Journal of*
20 543 *Climate*, 26(3), 726–739. <https://doi.org/10.1175/JCLI-D-12-00049.1>
21
22 544 Harris, I., Jones, P. D., Osborn, T. J., & Lister, D. H. (2014). Updated high-resolution grids of monthly
23 545 climatic observations – the CRU TS3.10 Dataset. *International Journal of Climatology*, 34(3),
24 546 623–642. <https://doi.org/10.1002/joc.3711>
25
26 547 Henley, B. J., Gergis, J., Karoly, D. J., Power, S., Kennedy, J., & Folland, C. K. (2015). A Tripole Index for
27 548 the Interdecadal Pacific Oscillation. *Climate Dynamics*, 45(11), 3077–3090.
28 549 <https://doi.org/10.1007/s00382-015-2525-1>
29
30 550 Hermanson, L., Ren, H.-L., Vellinga, M., Dunstone, N. D., Hyder, P., Ineson, S., Scaife, A. A., Smith, D.
31 551 M., Thompson, V., Tian, B., & Williams, K. D. (2018). Different types of drifts in two seasonal
32 552 forecast systems and their dependence on ENSO. *Climate Dynamics*, 51(4), 1411–1426.
33 553 <https://doi.org/10.1007/s00382-017-3962-9>
34
35 554 Huang, X., Zhou, T., Turner, A., Dai, A., Chen, X., Clark, R., Jiang, J., Man, W., Murphy, J., Rostron, J.,
36 555 Wu, B., Zhang, L., Zhang, W., & Zou, L. (2020). The Recent Decline and Recovery of Indian
37 556 Summer Monsoon Rainfall: Relative Roles of External Forcing and Internal Variability. *Journal of*
38 557 *Climate*, 33(12), 5035–5060. <https://doi.org/10.1175/JCLI-D-19-0833.1>
39
40 558 ICPO. (2011). Data and bias correction for decadal climate predictions. *International CLIVAR Project*
41 559 *Office Publication Series*, 150:5((Available online at [http://www.wcrp-](http://www.wcrp-climate.org/decadal/references/DCPP_Bias_Correction.pdf)
42 560 [climate.org/decadal/references/DCPP_Bias_Correction.pdf](http://www.wcrp-climate.org/decadal/references/DCPP_Bias_Correction.pdf))).
43
44 561 Jain, S., Scaife, A. A., & Mitra, A. K. (2019). Skill of Indian summer monsoon rainfall prediction in
45 562 multiple seasonal prediction systems. *Climate Dynamics*, 52(9), 5291–5301.
46 563 <https://doi.org/10.1007/s00382-018-4449-z>
47
48 564 Johnson, S. J., Turner, A., Woolnough, S., Martin, G., & MacLachlan, C. (2017). An assessment of
49 565 Indian monsoon seasonal forecasts and mechanisms underlying monsoon interannual
50 566 variability in the Met Office GloSea5-GC2 system. *Climate Dynamics*, 48(5), 1447–1465.
51 567 <https://doi.org/10.1007/s00382-016-3151-2>
52
53 568 Jones, C., Carvalho, L. M. V., & Liebmann, B. (2012). Forecast Skill of the South American Monsoon
54 569 System. *Journal of Climate*, 25(6), 1883–1889. <https://doi.org/10.1175/JCLI-D-11-00586.1>
55
56 570 Kanamitsu, M., Ebisuzaki, W., Woollen, J., Yang, S.-K., Hnilo, J. J., Fiorino, M., Potter, G. L., Kanamitsu,
57 571 M., Ebisuzaki, W., Woollen, J., Yang, S.-K., Hnilo, J. J., Fiorino, M., & Potter, G. L. (2002). NCEP–
58 572 DOE AMIP-II Reanalysis (R-2). *Bulletin of the American Meteorological Society*, 83(11), 1631–
59 573 1643. <https://doi.org/10.1175/BAMS-83-11-1631>
60

- 1
2
3 574 King, A. D., Hudson, D., Lim, E.-P., Marshall, A. G., Hendon, H. H., Lane, T. P., & Alves, O. (2020). Sub-
4 575 seasonal to seasonal prediction of rainfall extremes in Australia. *Quarterly Journal of the Royal*
5 576 *Meteorological Society*, 146(730), 2228–2249. <https://doi.org/https://doi.org/10.1002/qj.3789>
- 7 577 Kitoh, A., Endo, H., Krishna Kumar, K., Cavalcanti, I. F. A., Goswami, P., & Zhou, T. (2013). Monsoons
8 578 in a changing world: A regional perspective in a global context. *Journal of Geophysical*
9 579 *Research: Atmospheres*, 118(8), 3053–3065. <https://doi.org/10.1002/jgrd.50258>
- 11 580 Kuhlbrodt, T., Jones, C. G., Sellar, A., Storkey, D., Blockley, E., Stringer, M., Hill, R., Graham, T., Ridley,
12 581 J., Blaker, A., Calvert, D., Copsey, D., Ellis, R., Hewitt, H., Hyder, P., Ineson, S., Mulcahy, J.,
13 582 Siahann, A., & Walton, J. (2018). The Low-Resolution Version of HadGEM3 GC3.1: Development
14 583 and Evaluation for Global Climate. *Journal of Advances in Modeling Earth Systems*, 10(11),
15 584 2865–2888. <https://doi.org/10.1029/2018MS001370>
- 17 585 Lu, B., Scaife, A. A., Dunstone, N., Smith, D., Ren, H.-L., Liu, Y., & Eade, R. (2017). Skillful seasonal
18 586 predictions of winter precipitation over southern China. *Environmental Research Letters*, 12(7),
19 587 74021. <https://doi.org/10.1088/1748-9326/aa739a>
- 21 588 Martin, E. R., & Thorncroft, C. (2014). Sahel rainfall in multimodel CMIP5 decadal hindcasts.
22 589 *Geophysical Research Letters*, 41(6), 2169–2175. <https://doi.org/10.1002/2014GL059338>
- 24 590 Marvel, K., Biasutti, M., & Bonfils, C. (2020). Fingerprints of external forcing agents on Sahel rainfall:
25 591 aerosols, greenhouse gases, and model-observation discrepancies. *Environmental Research*
26 592 *Letters*, 15(8), 084023. <http://iopscience.iop.org/10.1088/1748-9326/ab858e>
- 28 593 Mauritsen, T., Bader, J., Becker, T., Behrens, J., Bittner, M., Brokopf, R., Brovkin, V., Claussen, M.,
29 594 Crueger, T., Esch, M., Fast, I., Fiedler, S., Fläschner, D., Gayler, V., Giorgetta, M., Goll, D. S.,
30 595 Haak, H., Hagemann, S., Hedemann, C., ... Roeckner, E. (2019). Developments in the MPI-M
31 596 Earth System Model version 1.2 (MPI-ESM1.2) and Its Response to Increasing CO₂. *Journal of*
32 597 *Advances in Modeling Earth Systems*, 11(4), 998–1038.
33 598 <https://doi.org/https://doi.org/10.1029/2018MS001400>
- 35 599 Mishra, S. K., Sahany, S., Salunke, P., Kang, I.-S., & Jain, S. (2018). Fidelity of CMIP5 multi-model
36 600 mean in assessing Indian monsoon simulations. *Npj Climate and Atmospheric Science*, 1(1), 39.
37 601 <https://doi.org/10.1038/s41612-018-0049-1>
- 39 602 Mohino, E., Keenlyside, N., & Pohlmann, H. (2016). Decadal prediction of Sahel rainfall: where does
40 603 the skill (or lack thereof) come from? *Climate Dynamics*, 47(11), 3593–3612.
41 604 <https://doi.org/10.1007/s00382-016-3416-9>
- 43 605 Monerie, P.-A., Robson, J., Dong, B., Dieppois, B., Pohl, B., & Dunstone, N. (2018). Predicting the
44 606 seasonal evolution of southern African summer precipitation in the DePreSys3 prediction
45 607 system. *Climate Dynamics*. <https://doi.org/10.1007/s00382-018-4526-3>
- 47 608 Monerie, P.-A., Robson, J. I., Dunstone, N. J., & Turner, A. G. (2021). Skillful seasonal predictions of
48 609 Global Monsoon summer precipitation with DePreSys3. *Environmental Research Letters*.
49 610 <http://iopscience.iop.org/article/10.1088/1748-9326/ac2a65>
- 51 611 Monerie, P.-A., Wilcox, L. J., & Turner, A. G. (2022). Effects of anthropogenic aerosol and greenhouse
52 612 gas emissions on Northern Hemisphere monsoon precipitation: mechanisms and uncertainty.
53 613 *Journal of Climate*, 1–66. <https://doi.org/10.1175/JCLI-D-21-0412.1>
- 55 614 Ndiaye, C. D., Mohino, E., Mignot, J., & Sall, S. M. (2022). On the detection of externally-forced
56 615 decadal modulations of the Sahel rainfall over the whole 20th century in the CMIP6 ensemble.
57 616 *Journal of Climate*, 1–51. <https://doi.org/10.1175/JCLI-D-21-0585.1>
- 59 617 Otero, N., Mohino, E., & Gaetani, M. (2016). Decadal prediction of Sahel rainfall using dynamics-

- 1
2
3 618 based indices. *Climate Dynamics*, 47(11), 3415–3431. [https://doi.org/10.1007/s00382-015-](https://doi.org/10.1007/s00382-015-2738-3)
4 619 2738-3
5
6 620 Parker, D., Folland, C., Scaife, A., Knight, J., Colman, A., Baines, P., & Dong, B. (2007). Decadal to
7 621 multidecadal variability and the climate change background. *Journal of Geophysical Research:*
8 622 *Atmospheres*, 112(D18). <https://doi.org/https://doi.org/10.1029/2007JD008411>
9
10 623 Schneider, U., Becker, A., Finger, P., Meyer-Christoffer, A., Ziese, M., & Rudolf, B. (2014). GPCP's new
11 624 land surface precipitation climatology based on quality-controlled in situ data and its role in
12 625 quantifying the global water cycle. *Theoretical and Applied Climatology*, 115(1–2), 15–40.
13 626 <https://doi.org/10.1007/s00704-013-0860-x>
14
15 627 Sheen, K. L., Smith, D. M., Dunstone, N. J., Eade, R., Rowell, D. P., & Vellinga, M. (2017). *Skilful*
16 628 *prediction of Sahel summer rainfall on inter-annual and multi-year timescales*. 8, 14966.
17 629 <http://dx.doi.org/10.1038/ncomms14966>
18
19 630 Shukla, J., & Paolino, D. A. (1983). The Southern Oscillation and Long-Range Forecasting of the
20 631 Summer Monsoon Rainfall over India. *Monthly Weather Review*, 111(9), 1830–1837.
21 632 [https://doi.org/10.1175/1520-0493\(1983\)111<1830:TSOALR>2.0.CO;2](https://doi.org/10.1175/1520-0493(1983)111<1830:TSOALR>2.0.CO;2)
22
23 633 Smith, D. M., Eade, R., Scaife, A. A., Caron, L.-P., Danabasoglu, G., DelSole, T. M., Delworth, T.,
24 634 Doblus-Reyes, F. J., Dunstone, N. J., Hermanson, L., Kharin, V., Kimoto, M., Merryfield, W. J.,
25 635 Mochizuki, T., Müller, W. A., Pohlmann, H., Yeager, S., & Yang, X. (2019). Robust skill of decadal
26 636 climate predictions. *Npj Climate and Atmospheric Science*, 2(1), 13.
27 637 <https://doi.org/10.1038/s41612-019-0071-y>
28
29 638 Sohn, S.-J., Tam, C.-Y., & Kug, J.-S. (2019). How does ENSO diversity limit the skill of tropical Pacific
30 639 precipitation forecasts in dynamical seasonal predictions? *Climate Dynamics*, 53(9), 5815–5831.
31 640 <https://doi.org/10.1007/s00382-019-04901-2>
32
33 641 Swart, N. C., Cole, J. N. S., Kharin, V. V., Lazare, M., Scinocca, J. F., Gillett, N. P., Anstey, J., Arora, V.,
34 642 Christian, J. R., Hanna, S., Jiao, Y., Lee, W. G., Majaess, F., Saenko, O. A., Seiler, C., Seinen, C.,
35 643 Shao, A., Sigmond, M., Solheim, L., ... Winter, B. (2019). The Canadian Earth System Model
36 644 version 5 (CanESM5.0.3). *Geoscientific Model Development*, 12(11), 4823–4873.
37 645 <https://doi.org/10.5194/gmd-12-4823-2019>
38
39 646 Tatebe, H., Ogura, T., Nitta, T., Komuro, Y., Ogochi, K., Takemura, T., Sudo, K., Sekiguchi, M., Abe, M.,
40 647 Saito, F., Chikira, M., Watanabe, S., Mori, M., Hirota, N., Kawatani, Y., Mochizuki, T., Yoshimura,
41 648 K., Takata, K., O'ishi, R., ... Kimoto, M. (2019). Description and basic evaluation of simulated
42 649 mean state, internal variability, and climate sensitivity in MIROC6. *Geoscientific Model*
43 650 *Development*, 12(7), 2727–2765. <https://doi.org/10.5194/gmd-12-2727-2019>
44
45 651 Turner, A. G., Inness, P. M., & Slingo, J. M. (2005). The role of the basic state in the ENSO–monsoon
46 652 relationship and implications for predictability. *Quarterly Journal of the Royal Meteorological*
47 653 *Society*, 131(607), 781–804. <https://doi.org/https://doi.org/10.1256/qj.04.70>
48
49 654 Walker, D. P., Birch, C. E., Marsham, J. H., Scaife, A. A., Graham, R. J., & Segele, Z. T. (2019). Skill of
50 655 dynamical and GHACOF consensus seasonal forecasts of East African rainfall. *Climate Dynamics*,
51 656 53(7), 4911–4935. <https://doi.org/10.1007/s00382-019-04835-9>
52
53 657 Wang, B., & Ding, Q. (2006). Changes in global monsoon precipitation over the past 56 years.
54 658 *Geophysical Research Letters*, 33(6). <https://doi.org/https://doi.org/10.1029/2005GL025347>
55
56 659 Wang, B., Kim, H.-J., Kikuchi, K., & Kitoh, A. (2011). Diagnostic metrics for evaluation of annual and
57 660 diurnal cycles. *Climate Dynamics*, 37(5), 941–955. <https://doi.org/10.1007/s00382-010-0877-0>
58
59 661 Wang, B., Li, J., Cane, M. A., Liu, J., Webster, P. J., Xiang, B., Kim, H.-M., Cao, J., & Ha, K.-J. (2018).

- 1
2
3 662 Toward Predicting Changes in the Land Monsoon Rainfall a Decade in Advance. *Journal of*
4 663 *Climate*, 31(7), 2699–2714. <https://doi.org/10.1175/JCLI-D-17-0521.1>
5
6 664 Wyser, K., van Noije, T., Yang, S., von Hardenberg, J., O'Donnell, D., & Döscher, R. (2020). On the
7 665 increased climate sensitivity in the EC-Earth model from CMIP5 to CMIP6. *Geoscientific Model*
8 666 *Development*, 13(8), 3465–3474. <https://doi.org/10.5194/gmd-13-3465-2020>
9
10 667 Yukimoto, S., Kawai, H., Koshiro, T., Oshima, N., Yoshida, K., Urakawa, S., Tsujino, H., Deushi, M.,
11 668 Tanaka, T., Hosaka, M., Yabu, S., Yoshimura, H., Shindo, E., Mizuta, R., Obata, A., Adachi, Y., &
12 669 Ishii, M. (2019). The Meteorological Research Institute Earth System Model Version 2.0, MRI-
13 670 ESM2.0: Description and Basic Evaluation of the Physical Component. *Journal of the*
14 671 *Meteorological Society of Japan. Ser. II*, 97(5), 931–965. <https://doi.org/10.2151/jmsj.2019-051>
15
16 672 Zhang, Z., Sun, X., & Yang, X.-Q. (2018). Understanding the interdecadal variability of East Asian
17 673 summer monsoon precipitation: Joint influence of three oceanic signals. *Journal of Climate*.
18 674 <https://doi.org/10.1175/JCLI-D-17-0657.1>
19

20 675
21
22 676
23
24
25
26
27
28
29
30
31
32
33
34
35
36
37
38
39
40
41
42
43
44
45
46
47
48
49
50
51
52
53
54
55
56
57
58
59
60